MODELING BEAMS WITH ELEMENTS IN PHASE SPACE[*]

E. M. Nelson

Los Alamos National Laboratory, Los Alamos, New Mexico 87545 USA

Abstract

Conventional particle codes represent beams as a collection of macroparticles. An alternative is to represent the beam as a collection of current carrying elements in phase space. While such a representation has limitations, it may be less noisy than a macroparticle model, and it may provide insights about the transport of space charge dominated beams which would otherwise be difficult to gain from macroparticle simulations.

The phase space element model of a beam is described, and progress toward an implementation and difficulties with this implementation are discussed. A simulation of an axisymmetric beam using 1d elements in phase space is demonstrated.

1 INTRODUCTION

Conventional particle codes represent beams as collections of macroparticles. This representation is adequate for many applications, but there are situations where relatively subtle details of the beam distribution are studied, and discretization noise in the macroparticle representation of the beam may obscure these details. Simulations of beam halo and emittance growth in space charge dominated beam transport are two examples. Algorithms which model a subset of the beam distribution have been successful. These include the δf algorithm[1, 2] and an algorithm[3] which employs a form of domain decomposition in phase space. Another approach is to model the Vlasov-Maxwell equation on a grid[4, 5]. Efforts using massively parallel computing paradigms with $\sim 10^8$ macroparticles are also providing significant advances in beam simulation[5].

This work discusses another model. In this model the beam is represented by a collection of elements in phase space instead of point-like macroparticles. Current is distributed over elements instead of being localized in macroparticles. This phase space element model of the beam represents a smooth phase space distribution better than a macroparticle model. Thus, this model might provide for beam transport calculations with less discretization noise. The motivation of this work is to develop improved models of emittance growth in DARHT[6].

2 PHASE SPACE ELEMENT MODEL

An element in phase space is a d dimensional simple shape embedded in a $2n$ dimensional phase space. The shapes are simplexes such as line segments, triangles or tetrahedra. Quadrilateral and hexahedral shapes may also be viable, as are shapes of four or more dimensions. Test particles at the element's vertices (and perhaps edges and faces) define the element's shape and location in phase space. Local coordinates are assigned to each point of phase space inside the element. There is a simple map from the element's local coordinates to global phase space coordinates.

Each element carries a number (or charge or current) density which is expressed in the element's local coordinate system. A number is obtained by integration of this density over the element's domain. In the jargon of differential geometry, the number density is a pseudo-d-form. This density is different from traditional densities where one integrates the density over a volume of configuration space to obtain a number.

The test particles evolve (e.g., over time) according to their equations of motion. The elements move with the test particles because each element's shape and location is defined by its test particles. The number density expressed in local coordinates on each element does not change. It is simply carried with the element. Collision-like effects are not being treated. The validity of this model depends on the interpolation of the evolved test particles being close to the evolution of an interpolated initial particle. Such tests can be performed to assess the accuracy of the model, and perhaps to adaptively refine the phase space elements which represent the beam.

3 AN IMPLEMENTATION

A code is being developed to model the transport of an intense steady-state axisymmetric beam in the presence of axisymmetric static fields. The phase space is $(x, y, ct, \gamma\beta_x, \gamma\beta_y, \gamma)$. The relativistic equations of motion for the particles are integrated in z. No paraxial approximation is used. Coordinates (x, y) are used instead of radius r to avoid potential difficulties pushing particles near the axis. Points (x, y) with the same radius r are equivalent. One can imagine revolving the phase space elements and particles about the axis in order to visualize the beam's particle distribution. Coordinate ct is computed for each particle, but this coordinate does not influence the particle motion.

The phase space elements are one dimensional line segments connecting two test particles. A local coordinate u, with $0 \leq u \leq 1$, labels points on each element. One test particle is $u = 0$ and the other is $u = 1$. The map from local coordinate u to global phase space coordinates is linear interpolation of the two test particles' phase space coordinates. Note that radius r is not linearly interpolated. It is computed from the interpolated values of x and y. This scheme better represents the beam's particles near the axis.
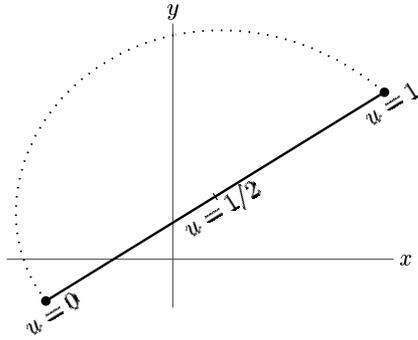
Figure 1: A one dimensional element (solid line) near the axis. Two test particles (filled circles) define the location and shape of the element. Local coordinate u identifies points on the element. The dotted line shows the effective element location if interpolation were performed in radius r instead of (x, y).

Fig. 1 illustrates a one dimensional element and the distinction among interpolation schemes.

An element's current density $\mathcal{J} = dI/du$ is a linear function of u. That is, the pseudo-one-form current density is $\mathcal{J} = (j_1 u + j_0) du$ with constants j_1 and j_0. This form for the current density $\mathcal{J}$ enables good representation of a uniform current density (traditional sense) beam.

The fields acting on the particles are external focusing fields, accelerating fields, and self-fields (including a flux conserving diamagnetic field). The self-fields are computed using Gauss' and Ampere's laws assuming the beam is uniform with respect to z. For example, Ampere's law gives

$$H_\theta(r) = \frac{I(r)}{2\pi r} = \frac{1}{2\pi r} \sum_i \int_{\mathcal{U}_i(r)} \mathcal{J}_i \qquad (1)$$

where $I(r)$ is the current enclosed by a circle of radius r, and i is a phase space element index. For the ith element, the domain of integration $\mathcal{U}_i(r)$ is the portion of the element inside of radius r,

$$\mathcal{U}_i(r) = \{u : 0 \le u \le 1, r_i(u) < r\}. \qquad (2)$$

The radius at u in the ith element is $r_i(u)$. An example is shown in Fig. 2. Notice that an element may have two intersections with the circle of radius r. The implementation splits elements into subelements during each self field calculation so that each subelement has at most one intersection with a circle.

Algorithms have been developed for higher dimensional phase space elements. Elements are first split into subelements so that intersections with circles are simple. A circle splits a triangle subelement into a triangular piece and a quadrilateral piece. The possibility that the triangle element encloses the axis has also been considered. A tetrahedral subelement splits into a tetrahedral piece and a prism piece, or into two prism pieces.

The motivation for using Gauss' and Ampere's law is to employ the simplest algorithm at this stage of the investi-
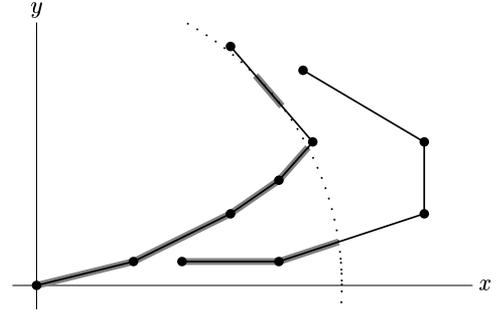

Figure 2: A collection of one dimensional phase space elements. For the self field calculation at the radius of the dotted circle, the current density is integrated over the region outlined in gray.

gation. The integration in Gauss' and Ampere's law does not scale well with increasing number of phase space elements and test particles. However, the integration requires calculation of the intersection of elements with only one circle at a time. A better implementation will use a grid for the computation of self-fields, but such an implementation will have to deal with intersections of an element with two circles instead of just one. This adds complexity to the code.

Accelerating fields are treated crudely at this time. A fixed $\Delta\gamma$ is added to each test particle as it passes through a gap. The magnetic field on-axis is computed from a rational function approximation. Off-axis fields are computed using a four term Taylor's expansion. The equations of motion for the test particles are integrated using a fourth order Runge-Kutta algorithm.

4 AN EXAMPLE

An example is shown in Figs. 3-5. Nominal DARHT-I parameters are employed except for the beam's initial emittance. The beam is not matched with the accelerator. The initial beam is a laminar (zero emittance), uniform current density beam. The particle energies are corrected for space charge depression and all particles have zero canonical angular momentum. The initial beam is composed of 100 elements equally spaced in radius on the positive x-axis.

The example illustrates two issues. First, the beam model is wrapping itself around the axis. This will ultimately ruin the effectiveness of the element's interpolation scheme. The wrapping has two sources. One is the tune shift due to the beam's self-fields. The other is the non-conservation of canonical angular momentum, p_θ, introduced mainly by the self-field calculation scheme.

The assumption of uniformity with respect to z in the self-field calculation leads to errors in p_θ. The error for particles near the axis are opposite in sign from the error for particles near the beam edge. Using an improved self-field calculation or particle pushing scheme will reduce this effect, but the tune shift must still be dealt with when the
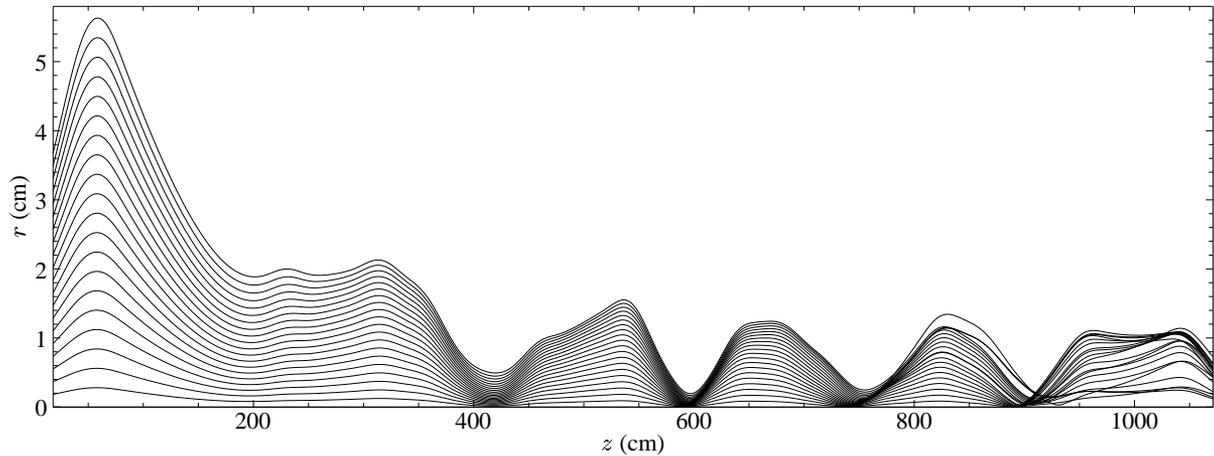
Figure 3: Trajectories of 20 particles (every 5th particle) of a mismatched laminar beam in the first 10 m of DARHT-I.
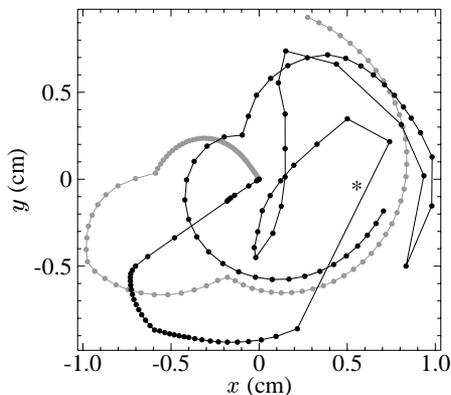

Figure 4: Configuration of the phase space elements of the beam at z=8.1 m (gray) and z=10 m (black). The gray curve clearly shows the beam model wrapping around the axis. The black curve shows that the model becomes very convoluted.

Figure 5: The beam model at z=8.1 m (gray) and z=10 m (black) projected onto the r-$\gamma\beta_r$ plane.

full accelerator is modeled.

One might modify the equations of motion to cancel the tune shift. Recall that the test particles in this axisymmetric simulation represent an equivalence class of particles at the same radius, so it is not absolutely necessary for their trajectories to coincide with real particles.

This leads to the second issue. The configuration of the beam at z=10 m (see Fig. 4) is quite convoluted. This casts doubt on the validity of the beam model. In fact, refinement of the model (i.e., more elements) shows that it is surprisingly good except near the large phase space element labeled *.

5   CONCLUSION

Some progress has been made in developing a phase space element model for a beam. More work is needed before this model's viability can be demonstrated concretely, but there are promising indications that the model will yield some improved beam simulations.
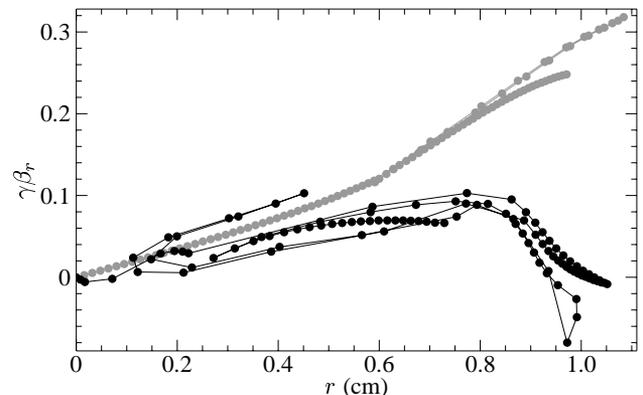
6   REFERENCES

[1] J. K. Coga and T. Tajima, "The δf Algorithm for Beam Dynamics," J. Comp. Phys. 116, 314-329 (1995).

[2] W. W. Lee, Q. Qian and R. C. Davidson, "Stability and Transport Properties of an Intense Ion Beam Propagating Through an Alternating Gradient Focusing Lattice," Phys. Lett. A 230, 347-352 (1997).

[3] T. Chen, J. Irwin and R. Siemann, "Simulation of the Beam Halo from the Beam-Beam Interaction," Phys. Rev. E. 49 (3), 2323-2328 (1994).

[4] A. Piquemal, "Renoir, a Numerical Simulation Code for the Study of Halo in Intense Charged Particle Beams," 1996 Computational Accelerator Physics, Williamsburg, VA, September 24-27, 1996, 137-142 (1997).

[5] R. Ryne and S. Habib, "Parallel Beam Dynamics Calculations on High Performance Computers," 1996 Computational Accelerator Physics, Williamsburg, VA, September 24-27, 1996, 377-388 (1997).

[6] M. J. Burns et al, "Status of the Dual-Axis Radiographic Hydrotest Facility," Proceedings of LINAC96, CERN, August 26-30, 1996, 875-877 (1996).